Journal of Power Sources 477 (2020) 228680

Contents lists available at ScienceDirect

Journal of Power Sources

journal homepage: www.elsevier.com/locate/jpowsour

Fiber-supported alumina separator for achieving high rate of high-temperature lithium-ion batteries

Yizheng Liu [a], Xiu Shen [b], Xin Wang [b], Longqing Peng [b], Texiong Hu [a], Peng Zhang [a,**], Jinbao Zhao [a,b,*]

[a] *College of Energy, Xiamen University, Xiamen, 361005, PR China*

[b] *State Key Lab of Physical Chemistry of Solid Surfaces, Collaborative Innovation Centre of Chemistry for Energy Materials, Engineering Research Center of Electrochemical Technology, Ministry of Education, State Province Joint Engineering Laboratory of Power Source Technology for New Energy Vehicle, College of Chemistry and Chemical Engineering, Xiamen University, Xiamen, 361005, PR China*

HIGHLIGHTS

- Thermally stable temperature above 800 °C.
- Pure inorganic ceramic flexible separator was synthesized.
- Excellent wettability and high ionic conductivity at high temperature.
- Stable cycling of 200 cycles under a rate of 20C at 120 °C.
- Greatly shorten the charging time.

ARTICLE INFO

Keywords:
Fiber-supported
Ceramic separator
Lithium-ion batteries
High-temperature
High-rate
Flexible

ABSTRACT

More and more application scenarios of rechargeable batteries like lithium-ion batteries are set up in high-temperature environments, such as large-scale energy storage, aerospace, oil extraction industry, etc. Besides of electrolyte, the separator is also a vital part of the battery's sustainable operation at high temperature working condition, however traditional polyolefin separators and even ceramic-coated polyolefin separators have poor thermal stability. This article provides a fiber-supported aluminum oxide separator with improved flexibility and thermal stability because of the introduced flexible SiC fiber network skeleton. The ceramic separator exhibits electrochemical performance equivalent to commercial separators at room temperature. What's more, with high-temperature electrolyte system, its conductivity at 120 °C reaches 5.12 mS cm^{-1}, which is 3 times higher than that at room temperature, so that the $LiFePO_4$ half-cell has excellent rate performance that still maintains a specific capacity of 140 mAh g^{-1} for 200 cycles under a rate of 20C at 120 °C. Specially, the half-cell containing the high temperature stable fiber-supported aluminum oxide separator realizes cycles of charging at a high temperature with high rate as 20C and discharging at a room temperature with normal rate of 1C, which is of great guiding significance to practical application.

1. Introduction

Lithium-ion batteries are widely used in all aspects of our life, such as digital field and electric vehicles due to their high energy density, high-rate charging/discharging capability, long cycle life, and environmental friendliness [1,2]. However, there are more and more application scenarios of lithium-ion batteries in high-temperature operation environments at present, such as aviation, petroleum industry, large-scale energy storage and electric vehicles in tropical regions. Furthermore, the kinetics of the electrochemical reaction as well as the ionic conduction of electrolyte could accelerate with the increase of operation temperature. It is reported that compared with the conductivity at room temperature, it will increase in multiples when the temperature increases above 100 °C [3]. In this way, the lithium-ion battery

---

* Corresponding author. College of Energy, Xiamen University, Xiamen, 361005, PR China.

** Corresponding author. College of Energy, Xiamen University, Xiamen, 361005, PR China.

E-mail addresses: pengzhang@xmu.edu.cn (P. Zhang), jbzhao@xmu.edu.cn (J. Zhao).

https://doi.org/10.1016/j.jpowsour.2020.228680
Received 23 April 2020; Received in revised form 26 June 2020; Accepted 19 July 2020

can operate at a higher rate meaning the high temperature lithium-ion battery also provides the possibility to further improve the power density and energy density of the battery. However, there is no doubt that it is important to develop novel materials capable of high performance at both ambient and elevated temperature operation condition. In the lithium ion battery, separator with high electronic insulation property, which separates the positive and negative electrodes, could keep apart the electrochemical reaction with gain and loss of electrons. This function not only works as the basis of the energy conversion between chemical energy and electric power of the cell, but also considered as a key issue of the safety to prevent the direct contact between the electrodes which could lead the energy conversion into producing heat [4,5]. Traditional polyolefin separators, such as polypropylene (PP), polyethylene (PE) boosted the commercialization of lithium-ion batteries because of their excellent mechanical properties, electrochemical stability and low cost of raw materials, but due to the low melting point (PE at 120 °C and PP at 160 °C) and the mechanical stretching manufacturing process, the thermal and dimensional stability of polyolefin separators at elevated temperature is not good enough for their broader application due to the limited operation temperature region and possible safety hazard [6]. It is well known that the thermal-induced shrinkage or melting of polyolefin porous membrane could cause direct contact of the two electrodes. And the resulted internal short circuit would accumulate heat and increase the temperature of the cell to initiate kinds of exothermic side reaction, finally leading to a thermal runaway. Additionally, the non-polarity of polyolefin separators exhibit poor wettability in the polar carbonate-based electrolyte solution [7,8] which also limits its performance of lithium-ion battery nowadays.

Among kinds of strategies, coating inorganic material such as Al_2O_3 [9], SiO_2 [10,11], TiO_2 [12] with high thermal tolerance onto the surface of a polyolefin separator to form a thin functional coating layer was regarded as a simple and effective method for improving the heat resistance and wetting performance [13–15]. A typical preparation process was coating nano-sized oxide powder with adhesive like CMC (Carboxymethyl Cellulose)-SBR (Styrene Butadiene Rubber) [9] or poly vinylidenefluoride-hexafluoro propylene copolymer (PVDF-HFP) [16] on both sides of polyethylene separator. Due to the presence of heat-resistant oxide particles with a high surface area in the coating layer, the composite membrane shows better thermal stability and improved wettability to organic liquid electrolytes compared to polyethylene separators. Furthermore, it is also possible to use a more heat-resistant polymer as a base film in combination with inorganic ceramic particles to improve heat shrinkage, coating a layer of Al_2O_3 ceramic on the surface of a polyimide (PI) membrane to improve high temperature stability [17]. In addition to coating with inorganic particles, polymer materials can also be used as a binder to make inorganic particle-based composite separators. The inorganic composite separator with coating layer composed of 94 wt% Al_2O_3 and 6 wt% polymer binder was kept at 130 °C for 40 min without almost any shrinkage [18]. Similarly, $MgAl_2O_4$ (magnesium aluminate) based porous ceramic membrane was prepared by using PVDF-HFP as a binder [19]. Electrospinning technology is also a suitable choice in the field of composite membranes [20]. PVDF-HFP fiber membranes were firstly obtained by electrospinning method, and then the composite separators obtained by coating the surface of the membrane with a layer of Al_2O_3 by ALD (Atomic layer deposition) technology, while this composite separator exhibited excellent thermal stability and fire resistance [21]. However, the above-mentioned ceramic coated separator or the separator modified by the ceramic filler has a large part of organic components, and it will still shrink to a certain extent under high temperature processing, especially in operando condition with a large amount of electrolyte which remains a great challenge to the safety performance of the battery and the sustainable operation of the battery at high temperature. Pure inorganic separators can completely ignore the effect of heat on the dimensional stability as well as the swollen effect of liquid electrolyte. But it is easy to notice that pure ceramic separators usually suffer from the poor flexibility, which brings a lot of inconvenience to battery manufacturing process and hinders the further commercialization.

Here, we introduced SiC fiber with both high flexibility and thermal stability as the matrix for Al_2O_3 nanoparticles to develop a novel flexible ceramic separator and applied it in a high temperature lithium ion battery. Firstly the Al_2O_3 slurry was casted onto the SiC fiber mat, and then remove organic binder at high temperature to obtain the SiC fiber-supported alumina separator (A@S ceramic separator). Here, A@S ceramic separator not only exhibits electrochemical performance equivalent to commercial separators at room temperature, but also shows excellent high-temperature stability. Additionally, it shows flexibility because of its flexible SiC fiber network skeleton, which also benefits to actual battery production. The A@S ceramic separator with high thermal stability provide a possibility to operate the electrochemical reaction of the cell at high temperatures to obtain a much better charge/discharge performance [6]. Further investigation revealed that the conductivity will increase greatly with the temperature increasing when it used together with a typical high temperature electrolyte system 1 M LiDFOB (Lithium difluoro (oxalato) borate)/PC (propylene carbonate). It exhibits excellent cycle performance at high temperatures of 120 °C with high rate. In particular, the half-cell battery realized cycles of charging at a high temperature of 20C and discharging at a room temperature of 1C. This should be a great guiding significance to practical application. On one hand, the battery can be used with further improved safety, on the other hand, the battery also could be discharged at room temperature and charged at high temperature which would greatly shorten the charging time and provide a new mode for promoting electric vehicle application.

2. Experiment

2.1. Preparation of the A@S ceramic separator

0.081 g of pre-dispersed SiC staple fibers was added in a 500 ml flat-bottomed beaker, then uniformly disperse the SiC fibers in the 250 ml ethanol solvent with ultrasonic for 25 min. After removing of supernatant, the SiC short fiber support network was obtained by keeping in blast drying oven at 80 °C for 12 h. Then, 2.619 g Al_2O_3 powder (TAIMEI CHEMICALS CO., LTD) with diameter about 200 nm was added to a mixed solution of 3.2 g ethanol and 3.2 g *N,N*-dimethylformamide (DMF), 2 to 3 drops of triethanolamine were added dropwise as the dispersant, and then dispersed by magnetic stirring for 8 h. After that, 0.48 g polyvinyl butyral (PVB) and 0.18 g polyethylene glycol (PEG) were added as the binder and plasticizer respectively, and stirring was continued for 12 h to obtain a homogeneous slurry. Next, the slurry was gradually added to the square groove with flat bottom covered with SiC support network, after the slurry flowed smoothly, the square groove was laid on a flat-plate heater at 60 °C for 2 h to evaporate the solvent. The obtained SiC short fiber supported Al_2O_3 film was moulded into a round film with 18.5 mm in diameter. Finally, the round film was kept in a muffle furnace at 600 °C for 12 h to obtain A@S ceramic separator.

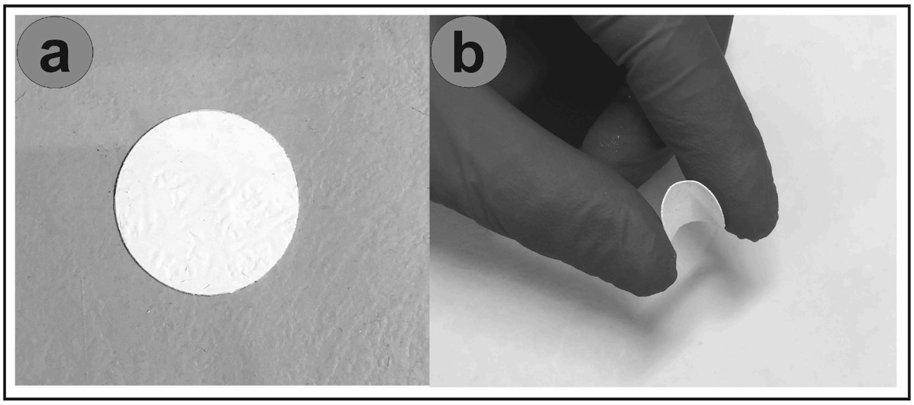

Fig. 1. a) A@S ceramic separator. b) The bending test of A@S ceramic separator.

2.2. Electrode preparation and cell assembly

The cathode material, including $LiFePO_4$ (Guoxian co. LTD China), acetylene black, and a polymer binder (9 wt% polyvinylidene fluoride (PVDF)), mixed with a weight ratio of 8: 1: 1, then used an automatic coating machine (Shanghai Modern Engineering Technique Co., Ltd) with a coating bar (150 μm) to coat the mixed slurry on the aluminum foil and dried under vacuum at 80 °C for 12 h. The thickness of the obtained coating layer is about 35 μm. The positive electrode material was cut into a 1.2 cm diameter wafer for assembling a coin cell, the loading of the LFP active material is around 2.68 mg cm^{-2}, and Li foil was used as the negative electrode when the battery was assembled. In room temperature experiments, commercial 301 electrolyte (EC/DMC = 1:1 (weight ratio) 1 mol L^{-1} $LiPF_6$, Zhangjiagang guotai huarong chemical new material co. LTD) was used. And 1 M LiDFOB dissolved in PC was used as the electrolyte in high temperature tests. All batteries were assembled in a glove box under an argon atmosphere.

2.3. Characterization of the A@S ceramic separator

The surface of the SiC fiber skeleton as well as the surface and cross-sectional morphology of the A@S ceramic separator were investigated by a field emission scanning electron microscope (FE-SEM, s-4800, Hitachi, Japan). XRD (MiniFlex 600, Rigaku, Japan) was used to monitor the phase of A@S ceramic separator. The porosity of A@S ceramic separator and Asahi PE diaphragms was tested by the n-butanol uptake method and calculated as follows:

$$\text{Porosity } \% = M_{BuOH} / (\rho_{BuOH} \times (M_{BuOH} / \rho_{BuOH} + M_m / \rho_P) \times 100\%$$

where ρ_{BuOH} and ρ_P represent the density of n-butanol and the separator, while M_{BuOH} and M_m represent the mass of n-butanol uptaked and the initial separator, respectively. A contact angle goniometer system (Powereach JC2000C1, Shanghai Zhongchen Digital Technique Equipment Co. Ltd., China) was used for the static contact angles text of A@S ceramic separator and Asahi PE separator. Thermogravimetric (TG) analyses of A@S ceramic separator and Asahi PE separator were performed using a STA 449 F3Jupiter thermal analyzer in air at a heating rate of 10 °C min^{-1} from 30 to 800 °C. The ionic conductivities of A@S

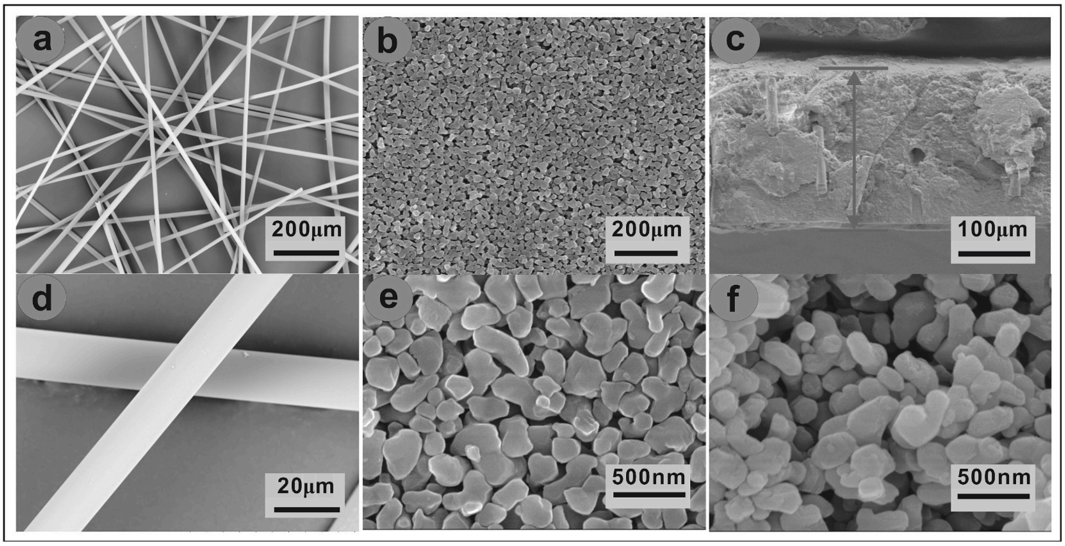

Fig. 2. a) d) The SEM image of SiC fiber network. The SEM image of A@S ceramic separator b) e) surface c) f) cross-section.

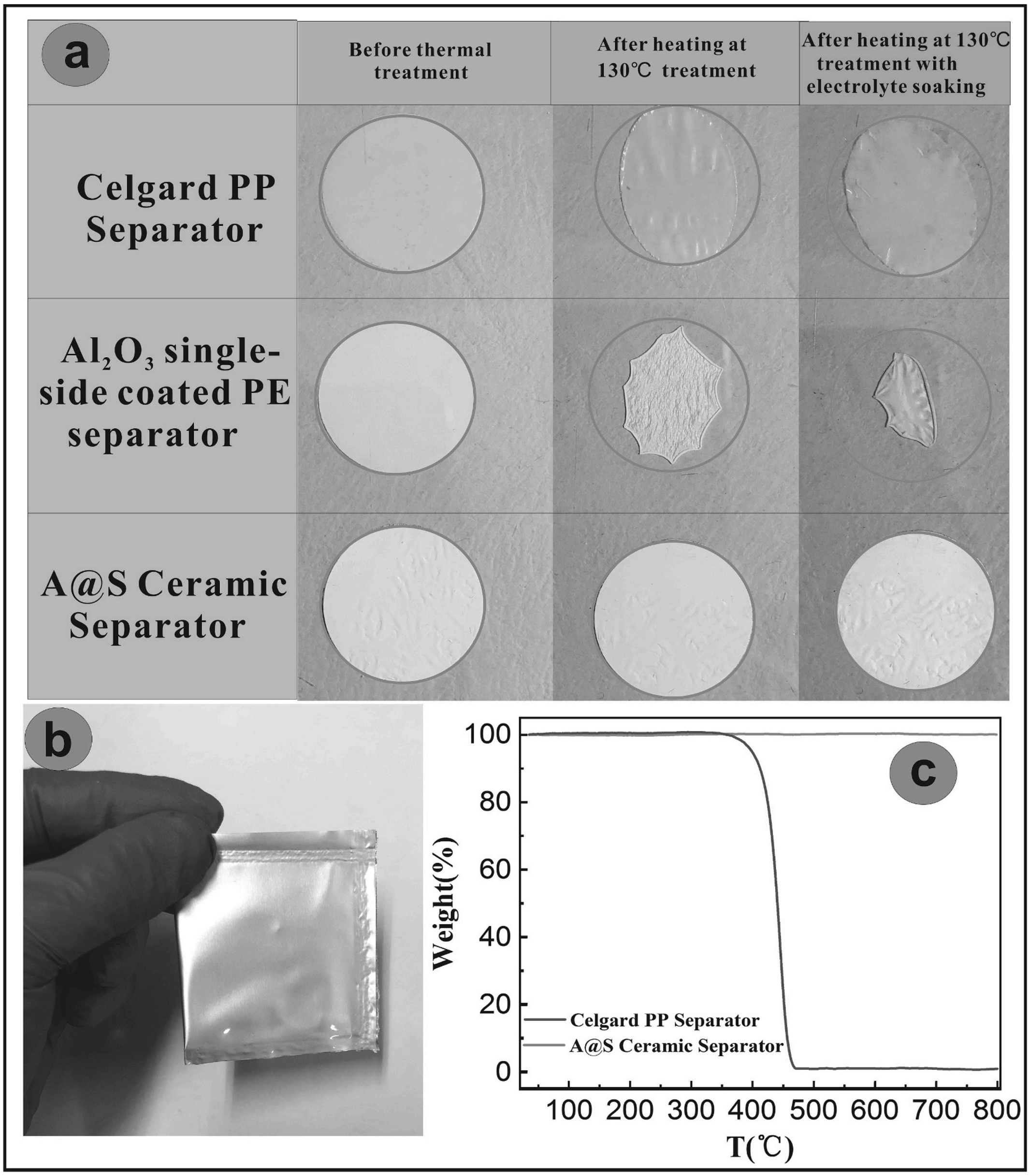

Fig. 3. a) The shrinkage of three different separators in different environments at 130 °C for 1 h. b) Separators sealed in an aluminum-plastic film bag. c) Thermogravimetric (TG) analyses of A@S ceramic separator and celgard PP separator.

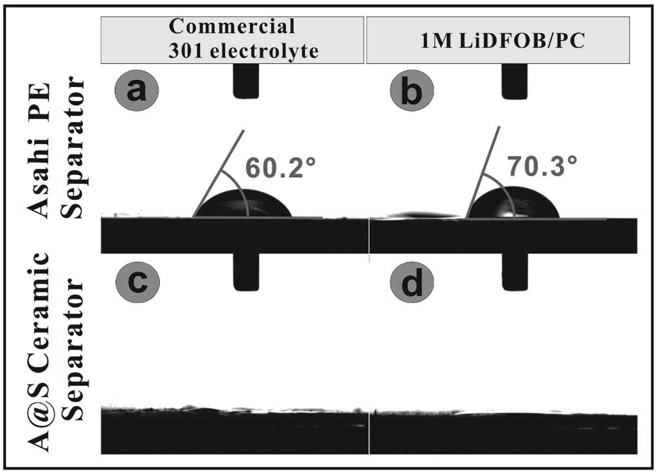

Fig. 4. Photographs of different electrolyte contact angles of A@S ceramic separator and Asahi PE separator.

ceramic separator and Asahi PE separator soaked with 301 electrolyte were investigated by electrochemical impedance spectroscopy using electrochemical workstation (Solartron, SI-1260, England) with the frequency range of 0.1 Hz–100 kHz. The linear sweep voltammograms (LSV) of Li/separator/stainless steel (SS) cell at a scan rate of 10 mV s^{-1} from 0 V to 6 V was measured in order to test the electrochemical stability of A@S ceramic separator and Asahi PE separator. Cells with A@S ceramic separator, Asahi PE separator and Celgard PP separator were prepared to investigate the cyclic and rate performance using the electrochemical test equipment (Newel, China). The cells were charged to 4 V and discharged to 2.5 V vs. Li/Li^+ with different rate from 0.2C to 5C and different temperature at room temperature and 120 °C. The high temperature battery cycling test was operated in an oven, and the battery was kept in a 120 °C incubator for 40 min before cycling, then charged to 4 V and discharged to 2.5 V vs. Li/Li^+ with different rate from 0.5C to 34.5C at 120 °C. In fact, as the most commonly applied separators in both commercial LIBs and academic research, Asahi PE and Celgard PP separators were treated as comparison of our ceramic separators throughout the experiment, and we explored the performance of both types of polyolefin separators and chose the better one to compare with our ceramic separators at room and high temperature respectively.

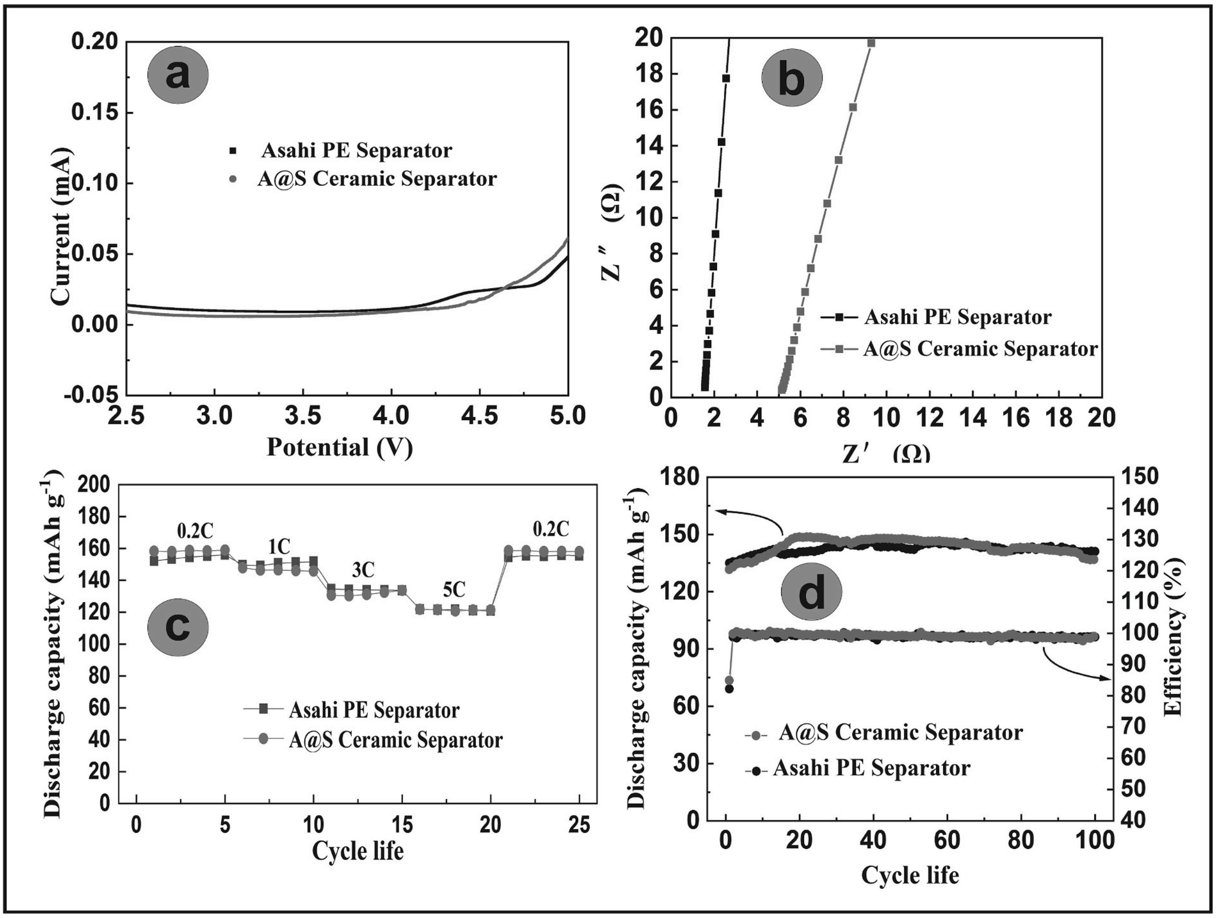

Fig. 5. a) The linear sweep voltammograms (LSV) test of A@S ceramic separator and Asahi PE separator. b) The Nyquist plots of Asahi PE separator and A@S ceramic separator. c) Rate performance in the LFP battery with 301 electrolyte at room temperature. d) Cycling performance in a half-cell of A@S ceramic separator and Asahi PE separator with 301 electrolyte at room temperature.

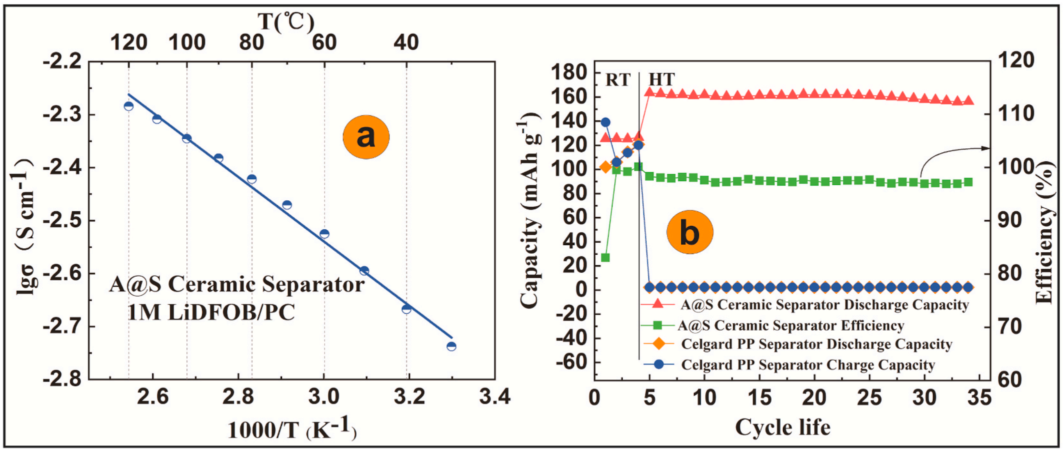

Fig. 6. a) The conductivity of A@S ceramic separator in 1 M LiDFOB/PC at different temperatures. b) Discharge capacity and coulombic efficiency of the A@S ceramic separator and Celgard PP separator at 0.5C under room temperature (25 °C) and high temperature (120 °C).

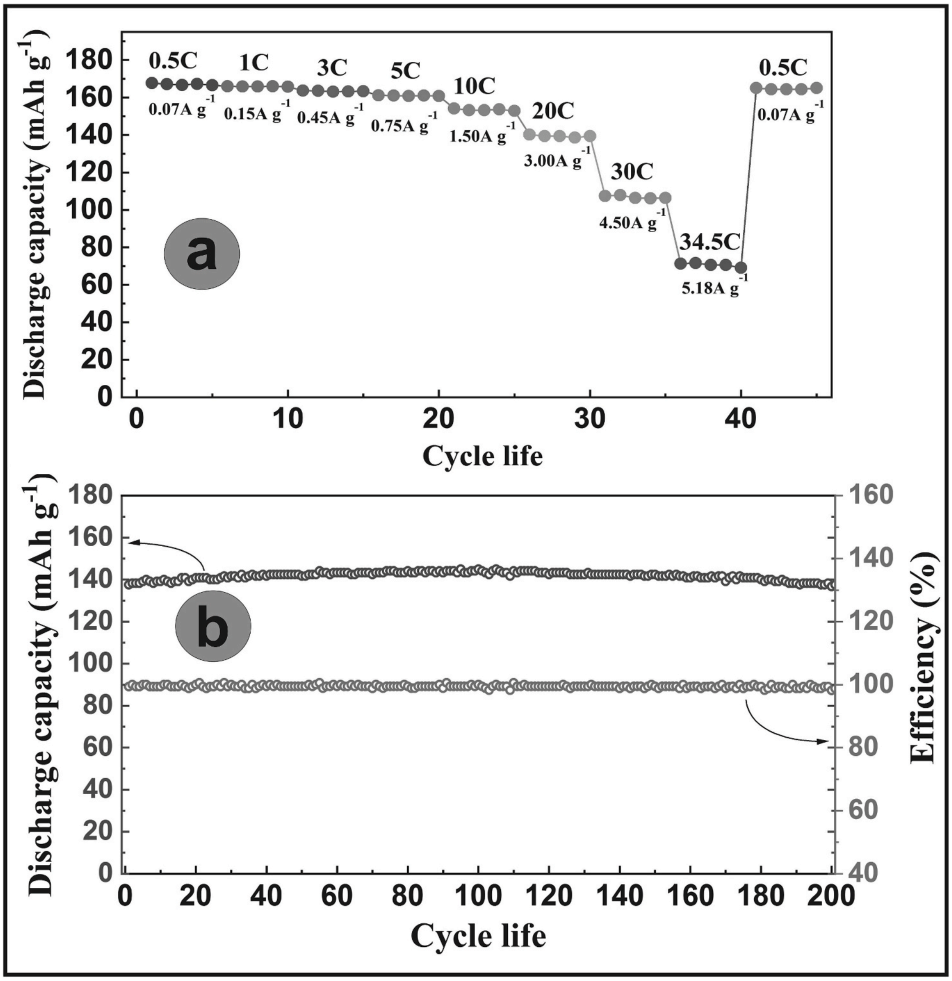

Fig. 7. a) Rate performance in the LFP battery of A@S ceramic separator under 120 °C. b) Discharge capacity and coulombic efficiency of the A@S ceramic separator at 20C under 120 °C.

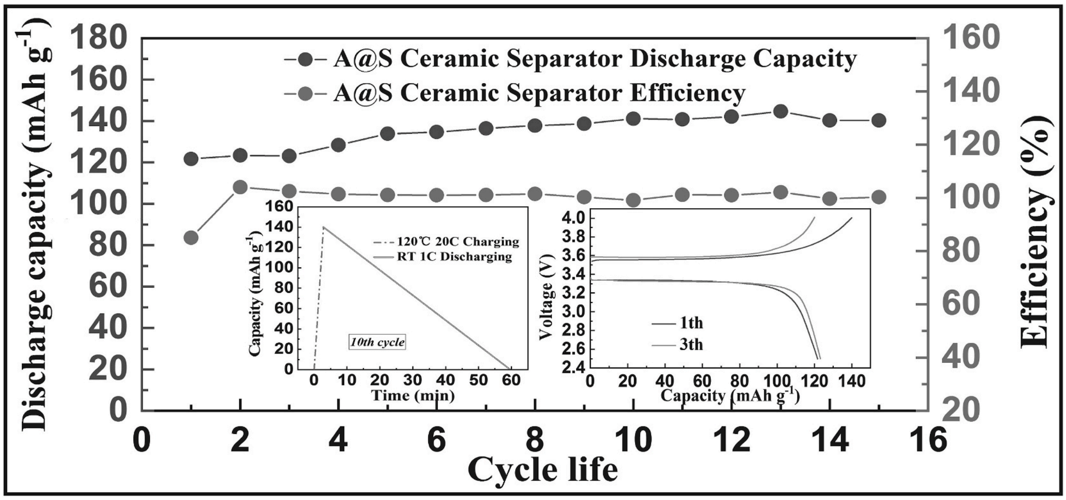

Fig. 8. Cycling performance of charging at 20C under 120 °C discharging it at 1C under room temperature including discharge capacity and coulombic efficiency of the A@S ceramic separator versus cycle life, the relationship between capacity and time in the tenth cycle (figure on the left) and the relationship between voltage and capacity in the first and third cycles (figure on the right).

3. Result and discussion

Fig. 1a exhibits the appearance of A@S ceramic separator made of SiC fiber buried in Al_2O_3 nano powders. The A@S ceramic separator is even white in colour and the SiC fiber could not be identified which means Al_2O_3 nano powders and SiC fiber were dispersed inside the separator. Furthermore, the obtained A@S ceramic separator could be bent over 90° without breakage as shown in Fig. 1b, which represents its excellent flexibility. It is undeniable that it apparently improves the poor flexibility of conventional inorganic ceramic separators which could be attributed to the introduction of SiC fiber network as the skeleton of the separator. A@S ceramic separator can maintain the integrity of the membrane after bending without peeling, crumble away and cracking, which is a prerequisite for its application in battery assembly process. The XRD pattern of the SiC fiber can be found in Fig. S1, the fiber is composed of β-SiC crystalline phase. SiC fiber network is composed of uniform SiC fiber with diameter of 10 μm and length of 2.5 mm which can be clearly identified from Fig. 2a and d. The aspect ratio of every single SiC fiber is as high as 250, and once formed a three dimensional network structure, it is easily to gain excellent flexibility due to the stress evenly distributed through the whole network. This could be also the fundamental reason for the overall flexibility of A@S ceramic separator by introducing SiC fiber as the skeleton of A@S ceramic separator. In addition, as a kind of atomic crystal, β-SiC itself also has excellent thermal stability with the decomposition temperature as high as 1600 °C which is much higher than polymer binder usually applied in ceramic separator. Both the high decomposition temperature of the β-SiC crystal and the three dimensional network structure make SiC fiber deal choice as the skeleton for construction a ceramic separator with superior flexibility and high thermal stability. Fig. S2 is the XRD pattern of A@S ceramic separator. It can be identified that the separator shows a pure α-Al_2O_3 phase without peaks of SiC fibers appearing. This may be due to the interior of the SiC fiber network embedded in the Al_2O_3 nanoparticles which are consistent with SEM image shown in Fig. 2c. Fig. 2b and e exhibit the surface morphology of the A@S ceramic separator. It can be seen that the surface is even and the nanoparticles are uniformly distributed while porous structure was formed by the Al_2O_3 nanoparticle stacking with the diameter about 200 nm. The porosity of 42.6% calculated by the n-butanol uptake method is very close to 43.1% of Asahi PE separator. On one hand, the porous structure could increase the electrolyte uptake of the separator leading to much more Li ions for ionic transport, while the channels through the interconnected pores would also promote Li ion conduction. Based on the large number and high mobility of charge carrier (Li ions) in the separator, it should gain a higher ionic conductivity when the separator is applied in the cell. On the other hand, the porous structure also enlarge the contact area between the Al_2O_3 nanoparticles and the polar solvent of the electrolyte which resulted the enhanced interaction between the separator and electrolyte. This may improve the electrolyte retention ability of the A@S separator which is also important for further improving the electrochemical and safety performance.

These pores and Fig. 2c and f shows cross-sectional morphology of A@S ceramic separator, the thickness of A@S ceramic separator is about 200 μm, and the SiC fiber is evenly distributed in the whole membrane. The thickness of the A@S ceramic separator could be optimized by adjusting the amounts and particle size of the Al_2O_3 powder (keep the mass ratio of Al_2O_3 and SiC constant), as shown in Fig. S3, adjusting the amount of Al_2O_3 to 3.492 g (Fig. S3a) and 2.328 g (Fig. S3b) to prepare A@S separators with different thickness. The amounts and proportion of Al_2O_3 powder given above in experimental section are the result of optimization in pre-experiment.

Whether a battery can work safely and continuously at high temperatures deeply depends on whether the separator can maintain dimensional stability at high temperatures. To investigate the thermal shrinkage of different separators including A@S ceramic separator, celgard PP separator and Al_2O_3-coated PE separator, they were all kept at 130 °C for 1 h. In particular, in order to be closer to the work environment of the battery, three types of separators were also impregnated with commercial 301 electrolyte and sealed in a bag of aluminum-plastic film, as shown in Fig. 3b. The thermal shrinkage results of three different separators in different environments with or without electrolyte soaking at 130 °C for 1 h is shown in Fig. 3a. It can be seen that Celgard PP separator has only one direction of shrinkage in the presence or absence of electrolyte infiltration. This result of the PP separator is related to the polypropylene material with a melting point higher than 130 °C and mechanically stretched manufacturing process. The Al_2O_3-coated PE separator exhibits more severe shrinkage when wetted by electrolyte than without electrolyte which may be due to the polymer binder used in the ceramic coating layer was swollen by the electrolyte solvent. By contrast, A@S ceramic separator in different environments shows no dimensional change. It can be concluded that the pure inorganic ceramic separator could completely overcome the high temperature resistance and even tolerate the high temperature resistance under the electrolyte infiltration. This improved thermal stability is very important for separator when practically applied in the lithium ion batteries.

For further studying the high temperature thermal stability of A@S ceramic separator, we performed a thermogravimetric analysis from room temperature to 800 °C, as shown in Fig. 3c. A@S ceramic separator exhibited excellent high-temperature thermal stability which has no mass change in the range of 800 °C. This is because it is composed of high-temperature stable Al_2O_3 powder and SiC fibers. It can theoretically withstand even high temperatures of 1200 °C; While the Celgard PP separator began to decompose at about 400 °C.

The electrolyte wettability is an important parameter for battery manufacturing. Conventional polymer separators have poor wettability with commercial polar electrolyte due to their non-polarity character. Poor wettability could also lead to low conductivity in the interface between electrode and electrolyte, which limits the electrochemical performance of lithium-ion batteries. The pure inorganic powder ceramic separator has excellent wettability due to the high affinity of oxide [6], which is an advantage for separator of lithium ion battery. Fig. 4 shows photographs of different electrolyte contact angles of A@S ceramic separator and Asahi PE separator. Commercial Asahi PE separator shows different affinity for different electrolytes, and the contact angles with the commercial 301 and 1 M LiDFOB/PC electrolyte are 60.2°, 70.3°, respectively. Specially, there was a larger contact angle with the electrolyte of the high temperature system due to use of pure high polarity solvent, which indicates that the wettability of the polyolefin separator towards high temperature electrolyte was even worse. In contrast, A@S ceramic separator had no selectivity to the electrolyte so that it can quickly absorb any electrolyte. Therefore, it can be concluded that it provides excellent wettability, which also helps to improve the interface characteristic to gain better electrochemical performance.

The linear sweep voltammograms (LSV) test of A@S ceramic separator and Asahi PE separator with stainless steel and Li electrode was used to investigate their electrochemical stability shown in Fig. 5a. The decomposition voltage of Asahi PE separator and commercial 301 system is about 4.3 V vs. Li/Li^+. In comparison, the decomposition voltage of system consisting of A@S ceramic separator and commercial 301 electrolyte is 4.5 V, which may be related to the removal of residual groups on the surface of the separator material through high-temperature calcination and the adsorption of impurities in the electrolyte by the Al_2O_3 nanoparticles. Fig. 5b shows the Nyquist plots for both liquid electrolyte-soaked Asahi PE separator and A@S ceramic separator. The ionic conductivity can be calculated by the equation: $\sigma = L/SR$, where R, S and L are the total resistance of the electrolyte across the separator and the area and thickness of the separator, respectively. The results show that the Asahi PE separator's ionic conductivity is 6.04×10^{-4} S cm^{-1} at 25 °C while the A@S ceramic separator is 4.21×10^{-3} S cm^{-1}. The higher ionic conductivity obtained by A@S ceramic separator can be ascribed to two main reasons: Firstly, the porous structure formed by the Al_2O_3 nanoparticles could on one hand increase the liquid electrolyte uptake thus increasing the number of the charge carrier for ionic conduction, on the other hand the pores with sub-micro diameter could also enlarge the contact area between the liquid electrolyte and the Al_2O_3 nanoparticles in the separator which enhances the interaction between them. Secondly, as well known that oxide nanoparticles such as Al_2O_3 normally used as the filler in polymer electrolyte could promote the ionic conduction through the interaction between the lithium salt and oxide nanoparticles [22]. It is believed that there is faster ionic conductive pathway on the surface of oxide nanoparticles. As a result, the A@S ceramic separator exhibit much higher ionic conductivity compared to the traditional polyolefin separator.

Before exploring the cycling performance in a LFP half-cell, we firstly made a pre-test of its rate performance in the battery, which is shown in Fig. 5c. For A@S ceramic separator, the specific capacity is 158.2 mAh g^{-1} at 0.2C. As the rate increases, the specific capacity decreases, and the capacity retention rates are 92.4%, 82.9%, 75.9% at 1C, 3C, and 5C, respectively. In addition, it can be found that it has a similar rate capacity as Asahi PE separator. Fig. 5d compares the cycle performance of the A@S ceramic separator and Asahi PE separator. The first cycle reversible efficiency of A@S ceramic separator and Asahi PE separator are 85.5% and 81.1%, respectively, which are related to the formation of SEI. It is caused by the reduced interface resistance due to the excellent wettability of the ceramic separator. In the subsequent cycles, the batteries with the two separators have similar cycle performance at 2C. After one hundred cycles, the capacity of 141.2 mAh g^{-1} is still maintained and the coulomb efficiency of each cycle is about 99.0%.

A@S ceramic separator is a stack of Al_2O_3 particles, so that porous structure acting as the channels for lithium ion conduction was formed between the particles. Because of the affinity of inorganic particles with liquid electrolyte, the conductivity of the A@S ceramic separator/301 electrolyte system is much higher than that of the Asahi PE separator/301 electrolyte. In the half-cell test at room temperature, the A@S ceramic separator is comparable to commercial polyolefin Asahi PE separators in the rate performance and cycle performance at 2C. In general, A@S ceramic separator has almost the same electrochemical performance as commercial Asahi PE separator at room temperature, which makes it possible to apply it to lithium ion batteries.

Even so, A@S ceramic separator shows more significant value by its remarkable performance at high temperature. Polyolefin separators have poor dimensional stability at high temperatures, especially under electrolyte soaking. It has been hoped that the introduction of ceramic particles can improve the high-temperature dimensional stability of polyolefin separators, but coating a layer of high-temperature-resistant ceramic particles does not significantly improve the heat resistance of polyolefin separators. Pure inorganic ceramic separators have attractive heat resistance, but their use is limited by poor flexibility. A@S ceramic separator, pure ceramic separator composed of Al_2O_3 and SiC solves the flexibility problem, which greatly helps its promotion and application. Obviously, A@S ceramic separator composed of high temperature resistant inorganic ceramics exhibits excellent high temperature dimensional stability, which provides solid foundation for the high-temperature lithium-ion batteries application.

Higher ionic conductivity is one of the advantages of high-temperature lithium-ion batteries. Fig. 6a shows the conductivity of A@S ceramic separator in 1 M LiDFOB/PC at different temperatures. At 120 °C, the conductivity (5.2×10^{-3} S cm^{-1}) of the system is 3 times of that at 30 °C (1.8×10^{-3} S cm^{-1}), and the conductivity in this temperature range increases with temperature increasing. The apparent activation energy $Ea = 11.64$ kJ mol^{-1} is obtained from the calculation from Arrhenius formula, in an other word, the lithium ion conduction in the A@S ceramic separator@1 M LiDFOB/PC electrolyte requires slightly lower energy than that of PP@1 M $LiPF_6$–EC/DMC electrolyte ($Ea = 13.757$ kJ mol^{-1}) [23]. Futhermore, the 0.5C rate cycling performance of the high-temperature half-cell is shown in Fig. 6b. In order to ensure the battery's activity before high temperature, we first did 4 cycles of charging and discharging at room temperature. As can be seen from the figure, celgard PP separator in 1 M LiDFOB/PC, the coulomb efficiency of the first cycle of the system at room temperature is 72.9% and the capacity of the first cycle is 100.2 mAh g^{-1}, the capacity of the fourth cycle is only 119.1 mAh g^{-1}. This is related to the low conductivity caused by the high viscosity of the PC at room temperature and the poor electrolyte wetting of the polyolefin separator. To make matters worse, when the battery is subjected to a high temperature cycle after being held at 120 °C for 3 h, the charge and discharge capacity of the battery where the celgard separator is located were reduced to zero due to a short circuit caused by the thermal shrinkage of the separator. In contrast, the battery where A@S ceramic separator was applied exhibited a coulomb efficiency of 83.1% on the first cycle at room temperature and a capacity of 125.5 mAh g^{-1} in the four cycles due to its excellent electrolyte wettability. The capacity increased to 161.4 mAh g^{-1}, and the coulomb efficiency remained at about 98.0% at 120 °C, which is due to the high conductivity of the electrolyte at 120 °C.

Furthermore, at the same time that the conductivity of the electrolyte is greatly improved at high temperatures, the kinetics of the electrochemical reaction during charge/discharge will also be accelerated, which provides conditions for high-rate charging and discharging of lithium-ion batteries. And our A@S ceramic separator provides a practical basis for the stable charge and discharge of lithium-ion batteries at high temperatures. In order to further explore the rate limit of the battery where A@S ceramic separator is located, we used a cathode material with a mass ratio of LFP: acetylene black: PVDF = 7: 2: 1 to reduce the low electron conductance effect of the LFP electrode material. The rate performance of a half-cell (loading of positive electrode 1.72 mg cm^{-2}) at 120 °C is shown in Fig. 7a. 0.5C, 1C, 3C, and 5C did not have a significant decrease in capacity with the rate increasing, and remain at about 163.2 mAh g^{-1}, which is due to high conductivity and faster electrode reaction dynamics at high temperatures. At 10C, 20C, 30C, 34.5C, the capacity is 153.3 mAh g^{-1}, 139.4 mAh g^{-1}, 106.6 mAh g^{-1}, and 70.5 mAh g^{-1}, respectively, and the capacity can be restored to 165.4 mAh g^{-1} after the rate is returned to 0.5C. Fig. 7b is the cycle performance of a battery containing A@S ceramic separator at a rate of 20C at 120 °C. The battery was activated at a low rate (2C) before. The capacity is maintained at 140.3 mAh g^{-1} at 20C and coulomb efficiency was above 99% through the whole cyclic process. It is true that these amazing results are not only due to the accelerated dynamics of electrode reaction at high temperature, but also related to the efficient and stable ionic conduction of the A@S ceramic separator and 1 M LiDFOB/PC system at high temperatures. But in a word, the superior thermal stability provide the solid foundation for the lithium ion battery operated at high temperature to gain faster ionic conduction and dynamics of electrode reaction thus promote this excellent electrochemical performance.

In the practical application scenarios, fast charging ability of the lithium ion battery should be paid more attention which could reduce the charging time for the electronic vehicle. Here we charged the battery at a rate of 20C at 120 °C and discharge it at 1C at room temperature to fit with an actual application scenario. The cycle results are shown in Fig. 8. The coulomb efficiency of the first cycle is 85.6%. Because the battery was not activated and charged and discharged directly, the capacity increases with the number of cycles. It reaches 139.8 mAh g^{-1} at the tenth cycle and remains stable with coulomb efficiency close to 100%. In the tenth cycle, the charge process only took 2.8 min to reach 139.8 mAh g^{-1} at 20C, and the discharge lasted 56.8 min at a rate of 1C. Fig. 8 also shows the relationship between voltage and capacity in the first and third cycles. The 120 °C charge voltage platform is 3.58 V at 20C, and the 1C discharge platform voltage at room temperature is 3.33 V. Here, we provide a probability to operate the lithium ion battery with high-temperature high-rate charging and normal-rate discharge at room temperature, combining high-temperature lithium-ion batteries with actual use, and the excellent performance of A@S ceramic separator is the key to achieving continuous battery stability.

4. Conclusion

In general, we have successfully fabricated a SiC fiber-supported Al_2O_3 ceramic separator, which exhibits excellent thermal stability, flexibility and electrolyte wettability. The lithium ion batteries with this ceramic separator show outstanding rate capability and cycle life at both room temperature and high temperature. In particular, at a high temperature of 120 °C, the LFP half-cell including the A@S ceramic separator system shows amazing rate performance and cycling performance at high rate. Moreover, the half-cell system achieves the cycle of 20C charging at 120 °C and 1C discharging at room temperature, which provides a feasible method for batteries with a wide range need of fast charging. In a word, A@S ceramic separator provides reliable components for the battery to work stably and continuously at high temperature condition as 120 °C. This benefit would greatly shorten the charging time and provide a new mode for promoting electric vehicle application.

CRediT authorship contribution statement

Yizheng Liu: Conceptualization, Methodology, Writing - original draft. **Xiu Shen:** Data curation, Writing - review & editing. **Xin Wang:** Data curation. **Longqing Peng:** Visualization. **Texiong Hu:** Investigation. **Peng Zhang:** Supervision, Writing - review & editing. **Jinbao Zhao:** Project administration, Funding acquisition.

Declaration of competing interest

The authors declare that they have no known competing financial interests or personal relationships that could have appeared to influence the work reported in this paper.

Acknowledgements

The authors gratefully acknowledge financial support from the National Natural Science Foundation of China [Grant Numbers 21875195, 21503180, 21621091], the Fundamental Research Funds for the Central Universities [Grant Number 20720170037] and the National Key Research and Development Program of China [Grant Number 2017YFB0102000].

Appendix A. Supplementary data

Supplementary data to this article can be found online at https://doi.org/10.1016/j.jpowsour.2020.228680.

References

[1] G.L. Zhu, K.C. Wen, W.Q. Lv, X.Z. Zhou, Y.C. Liang, F. Yang, Z.L. Chen, M.D. Zou, J. C. Li, Y.Q. Zhang, W.D. He, J. Power Sources 300 (2015) 29–40.
[2] E.S. Pampal, E. Stojanovska, B. Simon, A. Kilic, J. Power Sources 300 (2015) 199–215.
[3] R.R. Kohlmeyer, G.A. Horrocks, A.J. Blake, Z.N. Yu, B. Maruyama, H. Huang, M. F. Durstock, Nano Energy 64 (2019) 103927.
[4] H. Gwon, J. Hong, H. Kim, D.H. Seo, S. Jeon, K. Kang, Energy Environ. Sci. 7 (2) (2014) 538–551.
[5] H.-S. Jeong, J.H. Noh, C.-G. Hwang, S.H. Kim, S.-Y. Lee, Macromol. Chem. Phys. 211 (4) (2010) 420–425.
[6] M.N. He, X.J. Zhang, K.Y. Jiang, J. Wang, Y. Wang, ACS Appl. Mater. Interfaces 7 (1) (2015) 738–742.
[7] N.S. Choi, Y.M. Lee, J.H. Park, J.K. Park, J. Power Sources 119 (2003) 610–616.
[8] J.H. Choi, J. Jegal, W.N. Kim, J. Membr. Sci. 284 (1–2) (2006) 406–415.
[9] C. Shi, P. Zhang, L.X. Chen, P.T. Yang, J.B. Zhao, J. Power Sources 270 (2014) 547–553.
[10] D. Fu, B. Luan, S. Argue, M.N. Bureau, I.J. Davidson, J. Power Sources 206 (2012) 325–333.
[11] S.M. Kang, M.-H. Ryou, J.W. Choi, H. Lee, Chem. Mater. 24 (17) (2012) 3481–3485.
[12] H. Chen, Q. Lin, Q. Xu, Y. Yang, Z. Shao, Y. Wang, J. Membr. Sci. 458 (2014) 217–224.
[13] J.H. Park, W. Park, J.H. Kim, D. Ryoo, H.S. Kim, Y.U. Jeong, D.W. Kim, S.Y. Lee, J. Power Sources 196 (16) (2011) 7035–7038.
[14] K.J. Kim, J.-H. Kim, M.-S. Park, H.K. Kwon, H. Kim, Y.-J. Kim, J. Power Sources 198 (2012) 298–302.
[15] H.-S. Jeong, S.C. Hong, S.-Y. Lee, J. Membr. Sci. 364 (1) (2010) 177–182.
[16] W.-K. Shin, Y.-S. Lee, D.-W. Kim, J. Nanosci. Nanotechnol. 13 (5) (2013) 3705–3710.
[17] J. Lee, C.-L. Lee, K. Park, I.-D. Kim, J. Power Sources 248 (2014) 1211–1217.
[18] Y. Zhang, Z. Wang, H. Xiang, P. Shi, H. Wang, J. Membr. Sci. 509 (2016) 19–26.
[19] M. Raja, N. Angulakshmi, S. Thomas, T.P. Kumar, A.M. Stephan, J. Membr. Sci. 471 (2014) 103–109.
[20] Y. Xu, J.-W. Zhu, J.-B. Fang, X. Li, M. Yu, Y.-Z. Long, J. Nanomater. 2020 (2020) 3879040.
[21] X. Shen, C. Li, C. Shi, C. Yang, L. Deng, W. Zhang, L. Peng, J. Dai, D. Wu, P. Zhang, J. Zhao, Appl. Surf. Sci. 441 (2018) 165–173.
[22] F. Croce, L. Persi, B. Scrosati, F. Serraino-Fiory, E. Plichta, M.A. Hendrickson, Electrochim. Acta 46 (16) (2001) 2457–2461.
[23] C. Li, B. Qin, Y. Zhang, A. Varzi, S. Passerini, J. Wang, J. Dong, D. Zeng, Z. Liu, H. Cheng, Adv. Energy Mater. 9 (10) (2019) 1803422.